Testing the validity of Bose-Einstein statistics in molecules

P. Cancio Pastor,* I. Galli, G. Giusfredi, D. Mazzotti, and P. De Natale
Istituto Nazionale di Ottica (INO)–CNR and European Laboratory for Non-linear Spectroscopy (LENS), Via Carrara 1, 50019 Sesto Fiorentino FI, Italy
(Received 22 July 2015; published 11 December 2015)

The search for small violations of the validity of the symmetrization postulate and of the spin-statistics connection (SSC) has been addressed in the last four decades by experimental tests performed in different physical systems of identical fermions or bosons. In parallel and consequently, theories extending the quantum mechanics to a more general level have been proposed to explain such possible violations. In this paper, we present the most stringent test to a possible violation of the SSC under permutation of the bosonic ^{16}O nuclei in the $^{12}C^{16}O_2$ molecule. An upper limit of 3.8×10^{-12} for an SSC-anomalous CO_2 molecule is obtained using saturated-absorption cavity ring-down spectroscopy in the SSC-forbidden (00^01-00^00) $R(25)$ rovibrational transition of $^{12}C^{16}O_2$ at a 4.25-μm wavelength. Quantum mechanics implications of this result are discussed in the frame of the q-mutator theory. Finally, the perspective of stringent experimental tests of the symmetrization postulate in molecules that contain three or more identical nuclei is discussed.

DOI: 10.1103/PhysRevA.92.063820 PACS number(s): 42.50.Xa, 05.30.Jp, 33.20.−t, 42.62.Fi

I. INTRODUCTION

The symmetrization postulate (SP) and the Pauli exclusion principle (PEP) [or its more general formulation: the spin-statistics connection (SSC)] are fundamental quantum mechanics principles that form the basis for understanding the structure and stability of matter. The patterns observed in the periodic table, the discovery of color as a new hadronic degree of freedom, and the results of experiments on entanglement [1], on the indistinguishability of photons [2], on semiconductor physics [3], on Bose-Einstein condensation and degenerate quantum gases [4], and on cold-molecule chemistry [5] are just some of the evidence for the applicability of these principles in Nature. Therefore, it is important to investigate whether the principles are exact or whether deviations exist.

A large number of experiments, encompassing different physics fields and energies, have been performed to test the SSC and SP with a high precision, in both fermion and boson systems. In Table I, we report the most stringent ones (including the present work) [6–20]. They search for SSC-anomalous nuclear [10,12,14], atomic [6], or molecular [17–20] structures or SSC-forbidden nuclear [11,13] or atomic [7–9,15,16] transitions using different experimental spectroscopic techniques. For a survey of experiments related to possible violations of the SP and SSC and some speculations about why the SP and SSC might be violated and the theoretical issues beyond the, SP see [21] and [22].

An upper bound to possible violation is given in terms of the "symmetry-violation" parameter, β, where $\beta^2/2$ gives the probability that an antisymmetric (symmetric) component of a boson (fermion) system wave function will occur in a mixed state or the probability that when bosons (fermions) form a state, it will be strictly antisymmetric (symmetric). Its physical meaning and quantum-mechanical consequences depend on the particular system investigated and on the theoretical SP or SSC issues considered. Consequently, it is likely an oversimplification to use such a parameter to quantitatively compare the degree of violation in a wide variety of tests. It is worth noting that almost all the tests with fermions listed in Table I (except [6]), which achieve $\beta^2/2$ at the $10^{-28} - 10^{-35}$ level, can be considered one-particle tests of the identity of the tested fermion, a more general property of the particles, but not a test of their symmetry. Instead, tests on bosons (except [6] and [14], where systems with only two identical particles were investigated), are less well constrained. However, these simpler systems can be more easily modeled by theories to explain physical implications of possible symmetry violations (see Sec. IV for more details). Here, we report a new SSC test on the $^{12}C^{16}O_2$ molecule, which achieves $\beta^2/2 < 3.8 \times 10^{-12}$, the best reported so far for a system under permutation of two identical particles and the most stringent for possible small violations of Bose-Einstein statistics.

Taking into account that a composite system of an even number of fermions can be considered a single boson particle, small deviations of Bose-Einstein statistics can be measured with high-sensitivity spectroscopy of molecules containing two identical integer-spin nuclei. Spin-0 ^{16}O is an attractive nucleus for this kind of investigation because its relatively light mass leads to widely spaced molecular rotational levels without a hyperfine structure. Indeed, early experiments [17,18,24] investigated the spectrum of the $^{16}O_2$ molecule, searching for transitions between states that are antisymmetric under the exchange of the two nuclei and, hence, SSC anomalous. They used high-sensitivity laser absorption spectroscopy techniques developed in the near IR in the 1990s to set an upper bound of 5×10^{-8} to $\beta^2/2$. Improved tests were performed by investigating the spectrum of the $^{12}C^{16}O_2$ molecule in the near IR [19] and in the mid IR [20]. The last one established an upper limit for small violations of Bose-Einstein statistics, $\beta^2/2 < 1.7 \times 10^{-11}$, thanks to the combination of the low-noise non-linear-based coherent mid-IR source, laser wavelength modulation spectroscopy, and the high line intensity of the dipole rovibrational transitions of the ν_3 band of the CO_2 molecule around a 4.25-μm wavelength. Our present aim is to revisit this experiment with an improved sensitivity, provided by saturated-absorption cavity ring-down (SCAR) spectroscopy [25]. SCAR spectroscopy is a high-sensitivity

*pablo.canciopastor@ino.it

TABLE I. Symmetrization postulate and spin-statistics connection tests[a].

Particle (test)[b]	Field[c]	System	Process[d]	Method[e]	$\beta^2/2$ parameter	Ref. No(s).
Fermions						
e^- (PEP)	AP	^{4}He atoms	AAS-$[1s2s]_A\ ^1S_0\ ^4\check{H}e$	LS	$< 5 \times 10^{-6}$	[6]
e^- (PEP)	NP	Solid Cu	FAT-$e_I^- + Cu \rightarrow \check{C}u$[f]	x ray	$< 6 \times 10^{-29}$	[7,8]
e^- (PEP)	NP	Solid Pb	FAT-$e_F^- + Pb \rightarrow \check{P}b$[g]	x ray	$< 2.6 \times 10^{-39}$	[9]
p^+ (PEP)	AC	Sun	p-p bound state	H burning rate	$< 1.6 \times 10^{-15}$	[10]
p^+ (PEP)	NP	^{12}C	FNT-$^{12}C \rightarrow\ ^{12}\tilde{N} + \beta^- + \bar{\nu}_e$	β decay	$< 6.5 \times 10^{-34}$	[11]
p^+ (PEP)	AC	Primordial nucleosynthesis	ANS-$^5\tilde{L}i$	Estimation	$< 2 \times 10^{-28}$	[12]
p^+ (PEP)	NP	^{12}C	FNT-$^{12}C \rightarrow\ ^{12}\tilde{B} + \beta^+ + \nu_e$	β decay	$< 2.1 \times 10^{-35}$	[13]
Bosons						
n (SP)	AC	Supernova	ANS-$\tilde{O}$	AMS estimation	$< 1 \times 10^{-17}$	[14]
γ (SP)	AP	549-nm γ and Ba	F2γAT$-6s^2\ ^1S_0 \rightarrow 5d6d\ ^3S_1$	LS	$< 4 \times 10^{-11}$	[15,16]
^{16}O nuclei (SSC)	MP	$^{16}O_2$	AMoS-$X^3\Sigma_g^- v = 0\,(K = 2, J = 4)\ \widetilde{O_2}$	LS	$< 5 \times 10^{-8}$	[17,18]
^{16}O nuclei (SSC)	MP	$^{12}C^{16}O_2$	AMoS-$\Sigma_g^+ v = 0\,(J = 25)\ \widetilde{CO_2}$	LS	$< 2.1 \times 10^{-9}$	[19]
^{16}O nuclei (SSC)	MP	$^{12}C^{16}O_2$	AMoS-$\Sigma_g^+ v = 0\,(J = 25)\ \widetilde{CO_2}$	LS	$< 1.7 \times 10^{-11}$	[20]
^{16}O nuclei (SSC)	MP	$^{12}C^{16}O_2$	AMoS-$\Sigma_g^+ v = 0\,(J = 25)\ \widetilde{CO_2}$	LS-SCAR	$< 3.8 \times 10^{-12}$	This work

[a]Only the most stringent tests among different systems, processes, and experiments are included [23].
[b]SP, symmetrization postulate; SSC, spin-statistics connection; PEP, Pauli exclusion principle.
[c]NP, nuclear physics; AP, atomic physics; MP, molecular physics; AC, astrophysics-cosmology.
[d]ANS, anomalous nuclear structures; AAS, anomalous atomic structures; AMoS, anomalous molecular structures; FNT, forbidden nuclear transition; FAT, forbidden atomic transitions; F2γAT, forbidden two-photon atomic transition. A tilde, breve,or bracket over a symbol indicates, respectively, a nucleus, atom, or molecule with SP- and/or SSC-anomalous states.
[e]AMS, accelerator mass spectrometry; LS, laser spectroscopy; X ray, x-ray emission; β decay, β-decay emission.
[f]e_I^-: external electron injected into the metal.
[g]e_F^-: electron in the metal Fermi sea.

technique that we have recently developed and used to establish the record sensitivity of molecular detection in this spectral region, by measuring minimum detectable $^{14}C^{16}O_2$ pressures of 5×10^{-16} bar at a 4.5-μm wavelength [26,27].

As in [20], the present test looks for the forbidden (00^01-00^00) $R(25)$ rovibrational transition of $^{12}C^{16}O_2$ at 2367.265 cm^{-1}. The expected frequency of this transition, 70 968 804.973 MHz, was calculated with an uncertainty ranging from 0.3 to 3 MHz, taking into account the best rovibrational constants of the ν_3 band of the CO_2 molecule [28]. The wave function of the ground state of this transition is not allowed by the SSC, being antisymmetric under permutation of ^{16}O nuclei. Since electronic, vibrational, and nuclear-spin contributions to the ground-state wave function are permutation symmetric, the antisymmetric character must be given by the rotational contribution, which occurs for odd values of the rotational quantum number J. In particular, we investigate transitions from $J = 25$ because it is expected to be one of the most populated energy levels, taking into account the Boltzmann distribution of CO_2 molecules at room temperature. At the wavelength of 4.25-μm, dipole rovibrational transitions connecting the ground vibrational state to the antisymmetric stretching 00^01 vibrational state are allowed. Since the symmetry of the initial and final states of the system must be the same, the wave function of the excited state must, again, be permutation antisymmetric. This is satisfied for even J rotational states ($J = 26$ in our case) due to the antisymmetric character of the 00^01 state.

II. EXPERIMENT

SCAR spectroscopy of CO_2 transitions around 4.25 μm is performed with an experimental set-up described elsewhere [25,29]. Basically, cavity ring-down (CRD) signals are detected from a high-finesse Fabry-Perot (F-P) cavity, illuminated by IR laser radiation. When the IR frequency is resonant with a CO_2 molecular absorption, an increase in the CRD decay rate is measured, due to the additional intracavity losses caused by molecular absorption. If the absorption is saturated during part of the cavity decay, as in SCAR spectroscopy, the small gas absorption losses are measured separately from all the other cavity losses during each single CRD event, and the final sensitivity for molecular detection is increased.

The IR radiation is provided by an optical-frequency comb (OFC)–assisted difference-frequency-generation (DFG) continuous-wave coherent source [30]. The DFG process occurs inside the cavity of a Ti:sapphire laser operating around 850 nm (pump laser), single mode controlled by an injected extended-cavity diode laser. A Nd:YAG laser at 1064 nm, amplified up to 10 W using an Yb-doped fiber amplifier, provides the DFG signal laser. It is mixed with the intracavity Ti:sapphire radiation through a periodically poled lithium niobate nonlinear crystal. The frequency of the extended-cavity diode laser is phase-locked to the Nd:YAG frequency by direct digital synthesis, using the OFC to cover the frequency gap (about 71 THz) between the two continuous-wave lasers

[31]. In this way, the linewidth of the IR-generated radiation is given by a fraction of the narrow Nd:YAG linewidth (about 5 kHz in a 1-ms integration time), thus allowing a highly efficient coupling of the IR radiation to the F-P cavity. In addition, the Nd:YAG frequency is stabilized against the nearest tooth of the OFC. As a consequence, the IR frequency is absolutely traceable against the primary frequency standard with a precision of 6×10^{-13} in 1 s and an accuracy of 2×10^{-12}. Moreover, the intracavity DFG boosts the generated IR power up to 30 mW around a 4.3-μm wavelength, which provides the required power to saturate the CO_2 transitions.

The 1-m-long F-P cavity is formed by two high-reflectivity mirrors, each with a 6-m radius of curvature and optical losses of 590 ppm around 2367 cm^{-1}. Indeed, we measured an F-P finesse of about 5300 around this wavelength. A N_2-cooled InSb detector is used to detect the radiation transmitted by the cavity. When the F-P cavity is filled up to a predefined transmission threshold level, the input IR radiation is quickly switched off using an acousto-optic modulator on the DFG signal laser, and the CRD signal is detected. The SCAR absorption spectra are recorded by scanning the cavity-coupled IR frequency across the targeted transition. For each laser frequency, 20 consecutive SCAR-decay signals, each one resulting in an average of 1024 consecutive SCAR events, are stored for further analysis.

Pure carbon dioxide gas (99.999%) was used to fill the cavity at a pressure of 0.57 mbar. This value is a trade-off between the $^{12}C^{16}O_2$ concentration that maximizes the absorption at the target transition frequency and degradation of the cavity finesse due to the absorption from the wings of neighboring strong transitions. The gas was at room temperature (296 K). Under these conditions, the absorption-lineshape broadening is dominated by inhomogeneous processes, and the decay behavior of the intracavity power $P(t)$ is described by the differential equation [25]

$$\frac{dG(t)}{dt} = -\gamma_c G(t) - \gamma_g \frac{2}{1+\sqrt{1+G(t)}} G(t), \qquad (1)$$

where $G(t) = P(t)/P_S$ is the saturation parameter function, and P_S, γ_c, and γ_g are the saturation power of the targeted transition, the empty-cavity decay rate, and the gas absorption decay rate, respectively.

For each laser frequency, the recorded SCAR event is fitted by a numerical integration of Eq. (1), measuring the losses due to the gas absorption γ_g separately from the other losses γ_c. In this procedure, the saturation parameter at the beginning of the SCAR decay event, $G_0 = G(0) = P(0)/P_S$, was fixed to an appropriate value. More precisely, G_0 is factorized in two parameters: the amplitude of the SCAR signal and the saturation parameter corresponding to the cavity-transmitted power equivalent to a 1-V detected signal, G_0^{1V}. The former is a free parameter of the fit, whereas G_0^{1V} is kept fixed. In this way, amplitude variations of the decay signal are decoupled from the saturation effects. For the SSC test experiment, we assumed a G_0^{1V} parameter of 15 for the highly forbidden $R(25)$ transition, considering the gas temperature and the pressure conditions indicated above. It was estimated by measuring the intracavity power at 1 V of transmitted signal and by assuming a saturation process dominated by collisional rates in the transition-involved levels. This assumption is supported

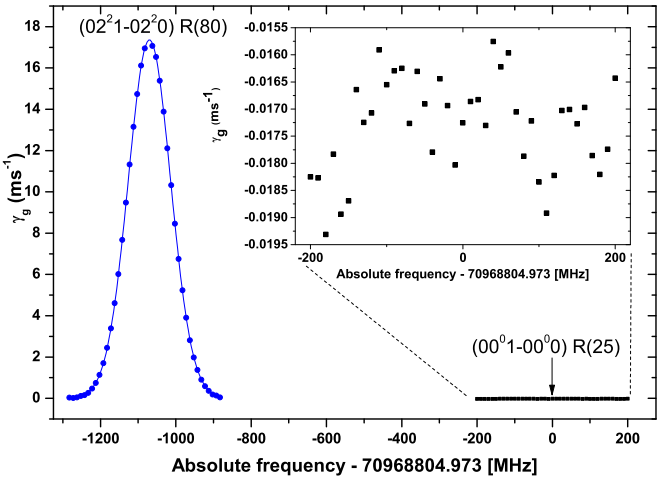

FIG. 1. (Color online) SCAR spectrum around the expected frequency of the SSC-forbidden (00^01-00^00) $R(25)$ transition of $^{12}C^{16}O_2$ at $P = 0.57$ mbar and $T = 296$ K. The SCAR spectrum of the (02^21-02^20) $R(80)$ $^{12}C^{16}O_2$ line at 2367.230 cm^{-1} and its Voigt fit with a fixed Doppler linewidth $\Delta\nu_D = 131.832$ MHz (FWHM) are also shown [solid (blue) curve with circles]. A single frequency scan was recorded in this case, with $G_0^{1V} = 33$. Fitted parameters were the line area $A_{R(80)} = 2471(3)$ ms^{-1} MHz, line center $\nu_0 = 70\,967\,749.216(46)$ MHz, and Lorentzian linewidth (FWHM) $\Gamma = 2.0(1)$ MHz. Inset: Vertical zoomed view of the portion ± 200 MHz around the $R(25)$ frequency. Two hundred laser frequency scans were averaged in this case, with $G_0^{1V} = 15$.

by the agreement between the estimated saturation intensity, evaluated by such criteria, and the measured one, performed on other CO_2 transitions of the same rovibrational band [32]. Nevertheless, the implication of this G_0^{1V} choice on the final uncertainty of the test is discussed in the following section. It is important to note that, in the framework of the present measurements, an adequate G_0^{1V} value minimizes the correlation between γ_g and γ_c decay rates, increasing the final precision [25,33].

In Fig. 1, the SCAR absorption spectrum around the $R(25)$ frequency is shown, which includes the nearby allowed (02^21-02^20) $R(80)$ $^{12}C^{16}O_2$ line at 2367.230 cm^{-1}. Details about the portion where $R(25)$ line absorption is expected are zoomed in on the inset. The experimental data points are the result of an average of 200 scans of the laser frequency, spanning 400 MHz around the $R(25)$ frequency, in 10-MHz steps. The OFC reference of these frequencies, and hence their precision and accuracy, allows a frequency reproducibility at the level of at least 2×10^{-12}, more than three orders of magnitude better than the best expected uncertainty quoted for the $R(25)$ frequency (0.3–3 MHz). As a consequence, the γ_g values measured at the same frequency of the scan can be statistically averaged, increasing the final sensitivity.

III. RESULTS

Observing the inset in Fig. 1, there is no visible evidence of any absorption above the noise level, which would be the hallmark of an SSC violation. More quantitatively, we estimate in this section the upper limit of a SSC violation by

measuring the maximum number of CO_2 molecules with the wrong symmetry that could absorb laser light considering the actual *S/N* ratio (see inset in Fig. 1).

In CRD experiments, and hence in the SCAR one, the gas absorption decay rate γ_g provides a precise measurement of the absorption coefficient α_g by using the simple relationship $\gamma_g = c\alpha_g$, where c is the velocity of light. This absorption coefficient (in cm^{-1}) is related to the other spectroscopic parameters of the molecular gas by

$$\alpha_g(\upsilon; P,T) = n_s S(T) \frac{\eta_0 P}{P_s} \frac{T_s}{T} g(\upsilon; P,T), \tag{2}$$

where n_s is the Loschmidt density (2.48×10^{19} cm^{-3}) at standard pressure $P_s = 1$ atm and temperature $T_s = 296$ K, $S(T)$ is the line intensity of the transition (in cm/molecule) at temperature T, $g(\upsilon; P,T)$ is the normalized lineshape, υ is the laser wave number (in cm^{-1}), and η_0 is the abundance of the targeted molecular species in the gas mixture at a total pressure P and temperature T (in atm and K, respectively). The latter parameter, which can assume a value between 0 and 1, is a direct measurement of the fraction of molecules in the gas mixture that contributes to the targeted absorption. Therefore, in the case of the present test, it can be considered an upper limit for $\beta^2/2$.

One method to estimate $\beta^2/2$ is to measure the absorption area under the proper line-shape function which fits the experimental data, leaving its center frequency and linewidth fixed [24], which, in terms of frequency ν, can be written as

$$\frac{\beta^2}{2} < \frac{1}{S_{R(25)}} \frac{1}{n_s} \frac{P_s}{P} \frac{T}{T_s} \int \frac{\alpha_g(\nu)}{c} d\nu. \tag{3}$$

Another option is to consider the root mean square (rms) noise in the spectral range where the forbidden line is expected [17,19], as a measurement of the absorption coefficient of a Doppler-broadened transition at the molecular frequency resonance,

$$\frac{\beta^2}{2} < \sqrt{\frac{\pi}{4\ln 2}} \frac{1}{S_{R(25)}} \frac{1}{n_s} \frac{P_s}{P} \frac{T}{T_s} \frac{\Delta\nu_D}{c} \alpha_g^{\mathrm{rms}}, \tag{4}$$

where $\Delta\nu_D$ is the Doppler full width at half-maximum (FWHM) Doppler and $S_{R(25)}$ is the calculated line intensity of the forbidden line, both at temperature T. This calculation can be easily performed using the known $S_{R(24)}$ value [20,34],

$$S_{R(25)}(T) \approx S_{R(24)}(T) \frac{26}{25} \exp\left(-\frac{50hB}{k_B T}\right), \tag{5}$$

where h is the Planck constant, k_B is the Boltzmann constant, and $B = 0.39$ cm^{-1} is the rotational constant for the ground vibrational state. We give both estimates below.

In Fig. 2, we have plotted the SCAR data around the expected $R(25)$ frequency in terms of α_g, as well as the fit to a Voigt function centered at this frequency and with $\Delta\nu_D = 131.834$ MHz (FWHM) at 296 K and a collisional broadening contribution $\Gamma = 3.187$ MHz (FWHM) [35]. A linear background is also considered in the fit curve. To test the validity of the chosen fitting function, the nearby $R(80)$ line was fitted, as shown in Fig. 1. We note the perfect agreement between the measured $\Gamma = 2.0(1)$ MHz (FWHM) from the fit and the calculated value [2.16(4) MHz (FWHM)], taking

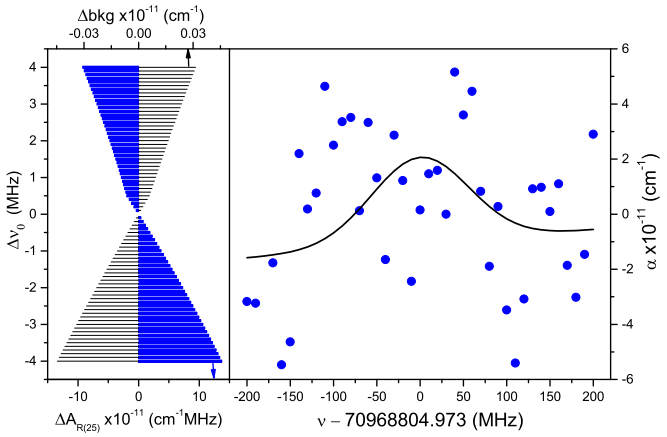

FIG. 2. (Color online) Absorption coefficient around the frequency of the SSC-forbidden (00^01-00^00) $R(25)$ $^{12}C^{16}O_2$ transition. Right: Filled (blue) circles, SCAR-measured data; solid (blue) line, Voigt fit to the expected absorption line-shape with $\Delta\nu_D = 131.834$ MHz (FWHM), $\Gamma = 3.230$ MHz (FWHM), and $\Delta\nu_0 = 0$ MHz. The measured Voigt area is $A_{R(25)}(0) = 4.5(3.6) \times 10^{-9}$ cm^{-1} MHz. Left: Thick (blue) bars, deviations of the measured area $\Delta A_{R(25)}$ (bottom scale); thin bars, deviations of the fit background Δbkg (top scale) for different fits performed by changing the line center frequency in the interval $\Delta\nu_0 = \pm 4$ MHz in 0.1-MHz steps. In both graphs, frequency scales are relative to the expected absolute frequency of the $R(25)$ line: 70 968 804.973 MHz.

into account the tabulated collisional broadening coefficient in the HITRAN database [34]. Moreover, the measured area gives a line-intensity determination of $S = 1.970(5) \times 10^{-25}$ cm/molecule, again in agreement with that known for this transition [$1.9(4) \times 10^{-25}$ cm/molecule] [34].

The measured area at zero detuning with respect to the $R(25)$ frequency, $A_{R(25)}(0) = 4.5(3.6) \times 10^{-9}$ cm^{-1} MHz, is a little bit higher than 1σ (standard deviation of the fit). Taking into account a line intensity $S_{R(25)}(296\ \mathrm{K}) = 2.65 \times 10^{-18}$ cm/molecule from Eq. (5), we can estimate from Eq. (3) an upper bound on the SSC violation of $\beta^2/2 < 4.1 \times 10^{-12}$. In order to evaluate possible systematic errors in this limit due to the uncertainty of the transition frequency, we performed different fits by moving the line center parameter of the $R(25)$ within an interval of ± 4 MHz (1 MHz larger than the estimated $\nu_{R(25)}$ uncertainty in the worst case). The deviations of the measured $A_{R(25)}$ of these fits with respect to the $A_{R(25)}(0)$ value ($\Delta A_{R(25)}$) are, at maximum, 0.15×10^{-9} cm^{-1}, well below the uncertainty in the measured area, as shown in the bar graph in Fig. 2. Thus, we can consider this systematic effect negligible at the present precision of the measured areas.

On the other hand, a calculation of the rms deviation of the measured α_g in the ± 200-MHz interval around $\nu_{R(25)}$ gives $\alpha_g^{\mathrm{rms}} = 3.0 \times 10^{-11}$ cm^{-1}, and using Eq. (4), we obtain $\beta^2/2 < 3.8 \times 10^{-12}$. In the SCAR experiment, the uncertainty of this upper bound depends on the value of G_0^{1V} used to fit the SCAR decays [Eq. (1)]. To understand its effect on the value of α_g^{rms}, we fitted the same SCAR decays with three G_0^{1V} values: 3.3, 33, and 330. The rms distribution for all these cases is shown in the left graph in Fig. 3. The standard deviation of such distributions scales approximatively with the factor

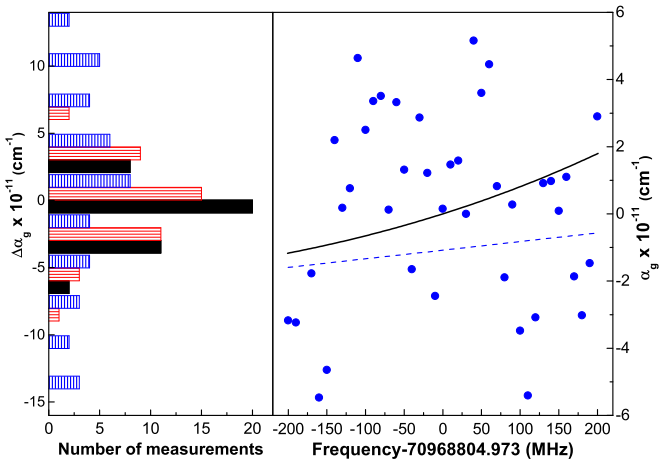

FIG. 3. (Color online) Sensitivity uncertainties in the SCAR test of the SSC. Left: Bar graph of the distribution of $\alpha_g(\nu)$ vs the mean value for $\nu = \pm 200$ MHz around $\nu_{R(25)} = 70\,968\,804.973$ MHz, for SCAR decays fitted with three G_0^{1V} values: 3.3 (black bars), 33 [vertical-striped (blue) bars], and 330 [horizontal-striped (red) bar]. Right: SCAR-measured data [filled (blue) circles] around $\nu_{R(25)}$ are compared with the linear fitted background [dashed (blue) line] and the residual absorption background [solid (black) line] due to the other CO_2 transitions in the interval 2366–2368 cm^{-1} with $S \geqslant 10^{-32}$ cm/molecule [34,36], properly shifted to be compared with the experiment on the same vertical scale (see text for more details).

$2/(1+\sqrt{1+G_0^{1V}})$. Although we are confident that the value of $G_0^{1V} = 15$ considered in this experiment allows effective saturation for the forbidden $R(25)$ transition, we estimated, at maximum, an error of a factor of 2 for this quantity, to take into account possible slower mechanisms of coherent relaxation between the involved levels, other than collisions. Such a G_0^{1V} uncertainty could give variation at a maximum of about 8% in the $\beta^2/2$ value measured from α_g^{rms}.

Both $\beta^2/2$ upper bound determinations described above are in agreement. The procedure described by Eq. (3) is a more stringent estimate of $\beta^2/2$, though more sensitive to small local fluctuations. Indeed, variations of the measured area for the fits performed at different detunings in the frequency interval ± 4 MHz follow the same behavior, but with opposite sign, as the background variations of such fits, as shown in the left graph in Fig. 2. Instead, the Eq. (4) approach gives a more conservative estimate, and hence, we take it as the upper bound of the SSC test for identical boson nuclei using SCAR spectroscopy.

We do not expect a significant improvement of these results by increasing the measurement time, thus averaging more SCAR data. Indeed, the absorption background around the frequency of the forbidden transition due to the strong wings of the allowed nearby lines limits the final sensitivity. In the right panel in Fig. 3, we show the simulated absorption (solid line), calculated using all the measured and known CO_2 lines with an S value down to 10^{-32} cm/molecule, in the 2366- to 2368-cm^{-1} interval [34,36]. In order to compare this simulation with the measured data in the same scale, the simulated values were shifted down by assigning to the simulated value of α_g at zero detuning the measured SCAR value, $\alpha_g(0)$. As shown, the behavior of this simulation is comparable to the residual absorption measured by SCAR, meaning that part of the absorption from other transitions is still present in the measured absorption coefficient. Although we have measured a SCAR sensitivity at the 10^{-14} level for detecting $^{14}CO_2$ at 4.5 μm, this absorbing background did not allow us to reach this limit.

Taking into account the upper bound $\beta^2/2 < 3.8 \times 10^{-12}$, the minimum detectable partial pressure of molecules in exchange-antisymmetric states with SCAR spectroscopy is lower than 2.1 fbar, corresponding to about 4.2×10^8 molecules in the total cell volume (about 8 liters). Considering that the IR beam occupies less than 1/1000 of this volume, the maximum number of molecules that could possess a symmetry-violating SSC is about 400 000. It is worth pointing out that this amount of molecules, and the related number of absorbed photons, still makes the absorption process stationary. This justifies the assumption of an inhomogeneous broadening mechanism to describe the absorbing process of the forbidden line.

IV. DISCUSSION AND CONCLUSIONS

The SCAR-measured $\beta^2/2$ value improves by more than four times the limit of our previous test [20]. It is, so far, the most stringent test of the SSC under permutation of bosons (see Table I), taking into account that the limit measured in [14] is subject to a high uncertainty due to its model dependence for determination of the neutron density in the supernova. Moreover, as pointed out in Sec. I, it is difficult to compare, in terms of quantum physical meaning, SP tests, which involve different numbers of identical particles that can undergo permutation.

Strictly speaking, all the SP-violation experiments that involve permutation of only two identical particles must be considered a test of the SSC rather than the SP. Indeed, the SP merely claims that all quantum states must be either totally symmetric or totally antisymmetric under exchange of identical particles, and it postulates that states with more complicated symmetries do not exist in Nature. Permutation symmetry in a system of only two identical particles is a one-dimensional problem which only allows symmetric or antisymmetric states as postulated by the SP. Several theories and speculations beyond the standard Bose-Einstein and Fermi-Dirac statistics (so-called "parastatistics" [21]) have tried to explain such possible SP violations, even though the SP makes no statement about a connection between the spin of the particles and the statistics as the SSC does. Among them, the q-mutator formalism [22] is the only quantum-field theoretical formalism that provides a description of "small" violations of the SP or SSC.

The q mutator is a generalization of the usual commutator and anticommutator relation between annihilation and creation operators,

$$a_m a_n^\dagger - q a_n^\dagger a_m = \delta_{mn}, \tag{6}$$

where q is a parameter that continuously turns Bose statistics ($q = 1$) into the Fermi one ($q = -1$), and vice versa. Particles satisfying Eq. (6) are called quons. "Small" deviations of the ordinary commutation or anticommutation algebra of standard statistical formalisms can be quantified in terms of $1 - |q|$. By assuming the validity of this algebra it has also been possible

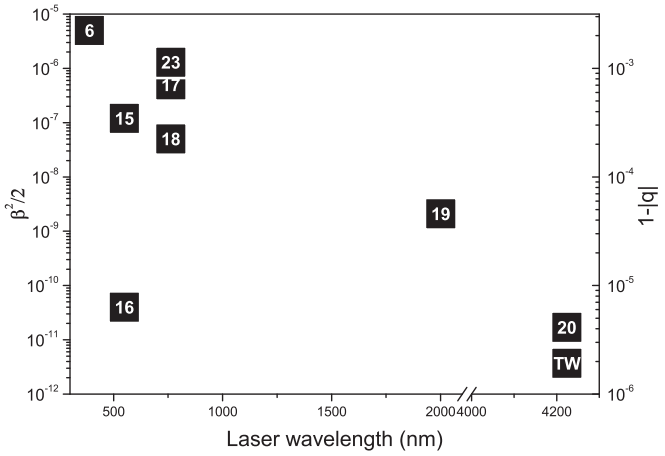

FIG. 4. Violation probabilities ($\beta^2/2$; left vertical scale) and q-formalism small deviations ($1-|q|$; right vertical scale) of the ordinary statistics from experimental tests of the SSC in systems with only two permuting identical particles and performed by atomic or molecular laser spectroscopy in the different spectral regions. Plotted numbers are reference numbers; TW, this work.

to translate the bound on the spin statistics for oxygen nuclei into a bound on the statistics of the nucleons composing the nuclei or, more generally, to establish a relationship between constraints on different kinds of particles. In Fig. 4, we show the comparison, in terms of such a parametrization, for all the experimental tests of the SSC listed in Table I for systems that involve only two exchange-identical particles. As demonstrated in [37] following a density matrix formalism for quons, the transition probabilities between SSC-anomalous states for two exchange-identical particles (i.e., the measured $\beta^2/2$) are proportional to $(1 \pm q)^2$, from which $1-|q|$ can be calculated. As shown, the present test allows us to determine the most stringent upper limit, to date, on possible violations of the SSC for bosons, namely, 1.9×10^{-6}.

Improving this limit by using high-sensitivity molecular spectroscopy of the CO_2 molecule will be a difficult challenge. Indeed, it is actually not limited by the spectroscopic technique, in this case SCAR spectroscopy, which was demonstrated to be sensitive at the level of a few tens of parts per quadrillion [26,27]. Even if it is performed with a F-P cavity of higher reflectivity at the wavelength of the present experiment, finesse degradation due to the residual absorption from even far-away tails belonging nearby transitions represents a plateau for the final achievable sensitivity. Other techniques, which avoid this background, should be conceived, to improve this result.

More interesting is to test the SP directly by using high-sensitivity molecular spectroscopy of simple molecules with three or more identical nuclei. Experiments with molecular candidates that contain three [38,39] or four [40,41] identical nuclei have been proposed, and some attempts have been performed in the latter case [41] but, unfortunately, with unpublished results. The simplicity of the spectra for the three-nuclei candidates has made them more appealing for experimental tests. In addition, the present technological advances in spectroscopic laser sources, emitting over almost all the electromagnetic spectrum, and the available high-sensitivity spectroscopic techniques could provide the stringent SP-violation tests proposed in those experiments. In particular, rovibrational spectroscopy of SO_3 in the IR by combining F-P-enhanced absorption spectroscopy techniques, such as SCAR, and quantum cascade laser sources could provide an upper SP-violation limit for bosons at the level of the present result of the SSC-violation upper bound in CO_2. On the other hand, from the theoretical point of view, systems that contain three or more identical composite nucleons can be treated within the q-mutator formalism, with the possibility of defining exotic symmetries as a smooth interpolation between symmetric and antisymmetric ones or statistics interpolating between the Bose and the Fermi cases.

ACKNOWLEDGMENTS

We acknowledge S. A. Tashkun and V. I. Perevalov for computing CO_2 transition frequencies and intensities around the targeted transition. This work was partially funded by ESFRI Roadmap, project "Extreme Light Infrastructure (ELI)", Italian Ministry of University and Research.

[1] S. Bose and D. Home, Phys. Rev. Lett. **88**, 050401 (2002).
[2] M. S. Kim, H. Jeong, A. Zavatta, V. Parigi, and M. Bellini, Phys. Rev. Lett. **101**, 260401 (2008).
[3] V. Y. Aleshkin, L. Reggiani, N. V. Alkeev, V. E. Lyubchenko, C. N. Ironside, J. M. L. Figueiredo, and C. R. Stanley, Semicond. Sci. Technol. **19**, S161 (2004).
[4] Z. Hadzibabic, Nat. Phys. **6**, 643 (2010).
[5] S. Ospelkaus, K.-K. Ni, D. Wang, M. H. G. de Miranda, B. Neyenhuis, G. Quéméner, P. S. Julienne, J. L. Bohn, D. S. Jin, and J. Ye, Science **327**, 853 (2010).
[6] K. Deilamian, J. D. Gillaspy, and D. E. Kelleher, Phys. Rev. Lett. **74**, 4787 (1995).
[7] S. Bartalucci *et al.*, Phys. Lett. B **641**, 18 (2006).
[8] C. Curceanu (Petrascu) *et al.*, Found. Phys. **41**, 282 (2011).
[9] S. Elliott, B. LaRoque, V. Gehman, M. Kidd, and M. Chen, Found. Phys. **42**, 1015 (2012).
[10] R. Plaga, Z. Phys. A **333**, 397 (1989).
[11] D. Kekez, A. Ljubičič, and B. Logan, Nature **348**, 224 (1990).
[12] M. H. Thoma and E. Nolte, Phys. Lett. B **291**, 484 (1992).
[13] G. Bellini *et al.* (Borexino Collaboration), Phys. Rev. C **81**, 034317 (2010).
[14] E. Baron, R. N. Mohapatra, and V. L. Teplitz, Phys. Rev. D **59**, 036003 (1999).
[15] D. DeMille, D. Budker, N. Derr, and E. Deveney, Phys. Rev. Lett. **83**, 3978 (1999).
[16] D. English, V. V. Yashchuk, and D. Budker, Phys. Rev. Lett. **104**, 253604 (2010).
[17] M. de Angelis, G. Gagliardi, L. Gianfrani, and G. M. Tino, Phys. Rev. Lett. **76**, 2840 (1996).

[18] L. Gianfrani, R. W. Fox, and L. Hollberg, J. Opt. Soc. Am. B **16**, 2247 (1999).
[19] G. Modugno, M. Inguscio, and G. M. Tino, Phys. Rev. Lett. **81**, 4790 (1998).
[20] D. Mazzotti, P. Cancio, G. Giusfredi, M. Inguscio, and P. De Natale, Phys. Rev. Lett. **86**, 1919 (2001).
[21] C. Curceanu, J. D. Gillaspy, and R. C. Hilborn, Am. J. Phys. **80**, 561 (2012).
[22] O. W. Greenberg, Phys. Rev. D **43**, 4111 (1991).
[23] Experiments which violate the supersymmetrization rule (i.e., those that involve transitions between states of different symmetry) are not considered SP or SSC tests. At best these experiments are tests of electron or nucleon stability.
[24] R. C. Hilborn and C. L. Yuca, Phys. Rev. Lett. **76**, 2844 (1996).
[25] G. Giusfredi, S. Bartalini, S. Borri, P. Cancio, I. Galli, D. Mazzotti, and P. De Natale, Phys. Rev. Lett. **104**, 110801 (2010).
[26] I. Galli, S. Bartalini, S. Borri, P. Cancio, D. Mazzotti, P. De Natale, and G. Giusfredi, Phys. Rev. Lett. **107**, 270802 (2011).
[27] I. Galli, S. Bartalini, P. Cancio, P. De Natale, D. Mazzotti, G. Giusfredi, M. E. Fedi, and P. A. Mandò, Radiocarbon **55**, 213 (2013).
[28] D. Long, G.-W. Truong, J. Hodges, and C. Miller, J. Quant. Spectrosc. Radiat. Transfer **130**, 112 (2013).
[29] P. Cancio, I. Galli, S. Bartalini, G. Giusfredi, D. Mazzotti, and P. De Natale, in *Cavity-Enhanced Spectroscopy and Sensing. Springer Series in Optical Sciences, Vol. 179*, edited by G. Gagliardi and H. P. Loock (Springer-Verlag, Berlin, 2014), pp. 143–162.
[30] I. Galli, S. Bartalini, S. Borri, P. Cancio, G. Giusfredi, D. Mazzotti, and P. De Natale, Opt. Lett. **35**, 3616 (2010).
[31] I. Galli, S. Bartalini, P. Cancio, G. Giusfredi, D. Mazzotti, and P. De Natale, Opt. Express **17**, 9582 (2009).
[32] D. Mazzotti, S. Borri, P. Cancio, G. Giusfredi, and P. De Natale, Opt. Lett. **27**, 1256 (2002).
[33] K. Lehmann, Appl. Phys. B **116**, 147 (2014).
[34] L. Rothman *et al.*, J. Quant. Spectrosc. Radiat. Transfer **130**, 4 (2013).
[35] Γ for the forbidden $R(25)$ line was calculated taking into account the self-collisional broadening coefficients reported for the nearby $R(24)$ and $R(26)$ allowed transitions [34].
[36] S. A. Tashkun and V. I. Perevalov (private communication).
[37] R. C. Hilborn, AIP Conf. Proc. **545**, 128 (2000).
[38] G. Modugno, D. Mazzotti, M. Modugno, N. Picqué, G. Giusfredi, P. C. Pastor, P. De Natale, and M. Inguscio, AIP Conf. Proc. **545**, 295 (2000).
[39] G. Modugno and M. Modugno, Phys. Rev. A **62**, 022115 (2000).
[40] G. M. Tino, AIP Conf. Proc. **545**, 260 (2000).
[41] C. J. Bordé and C. Chardonnet, AIP Conf. Proc. **545**, 274 (2000).